Acta Microscópica, Vol. 2, Nº 2, November 1993, pp 166 - 172

Hormone Granule Formation in the Golgi Complex of Pituitary Cells

Susan Tai[1], Victoria E. Centonze[2], Bernard Wentworth[3], and Ralph Albrecht[4]
[1] Fundación Instituto Metropolitano de Estudios Científicos (FIMEC) de la Universidad Nacional Experiemental Simón Rodríguez, Caracas, Venezuela (Fax: 582-979-7064) [2] IMR, University of Wisconsin, Madison, WI USA [3] Dept. of Poultry Science, University of Wisconsin, Madison, WI USA [4] Dept. of Animal Health and Biomedical Sciences, University of Wisconsin, Madison, WI USA

ABSTRACT

Frozen sections of turkey pituitary glands were processed for Confocal Laser Scanning Microscope (CLSM) observation.

Double labeling method was applied to those frozen samples. Sections were first incubated with a primary antibody (either rabbit anti-turkey growth hormone, GH or rabbit anti-turkey prolactin, PRL) and then incubated with Texas red anti-rabbit antiserum. After antibody incubations were completed, the sections were prepared for labeling with fluorescent ceramide.

Fluorescent imaging was performed using a CLSM, it reveals not only the distribution of GH and PRL cells, but also the spatial relationship of hormone granules and Golgi complex.

KEY WORDS

Laser scanning confocal microscopy, Turkey pituitary gland, Growth hormone cells, Prolactin secretory cells, fluorescent ceramide.

INTRODUCTION

The golgi complex participates in the process of pituitary hormone synthesis. Its function is to concentrate and package secretory materials released from the rough endoplasmic reticulum (rER) and form hormone granules in the trans cisternae of the golgi [8, 9, 28, 30].

Biochemical methods have been used in previous studies to isolate enzymes from different cisternae of the golgi stacks in order to ellucidate the function of the complex [3, 4, 7, 10, 11, 12, 13]. The ultrastructure of the elaborate subcellular organization of the golgi has also been studied by light microscopy (LM), transmission and scanning electron microscopy (TEM and SEM) and some specific components have been localized by autoradiography [2, 9, 16, 21, 31] and immunocytochemical methods [1, 15].

In a previous paper, we used conventional TEM, high voltage TEM, high resolution scanning electron microscopy (HR-SEM) and confocal laser scanning microscopy (CLSM) to demosntrate that the golgi complex of the chicken pituitary cell is one single structure. We showed that all of the golgi stacks within a single cell are interconnected [30].

TEM can only provide two dimentional information for structures observed in thin sections. HR-SEM does give a three dimensional perspective however it is limited to topographical structures. Our interest, at present, is to develop a method of observation that permits the visualization of the vital relationship between the hormone formation and the Golgi structure.

In 1983, Lipsky and Pagano [17] first reported that a fluorescent derivative of ceramide, N- (-7- nitrobenz - 2 - oxa - 1,3 - diazol - 4 - aminocaproyl) - D - erythro - sphingosine (C6-NBD - Cer), labels the Golgi complex of cells. Subsequent work by other investigators has demonstrated that several NBD - lipids behave

differently from one another with respect to their metabolism as well as their initial localization and redistribution in the subcellular membrane system [14, 18, 19, 22]. A fluorescent ceramide analogue thereby provides great advantages for molecular mapping of the Golgi intracellular configuration and organelle continuity. Pagano et al. [23] also demonstrated the use of ceramide for labeling fixed cells.

We have used ceramide to label Golgi in frozen pituitary tissue sections. This an invaluable method for specifically identifying Golgi in membrane rich regions where hormone granules are synthsized.

MATERIALS AND METHODS

A. Preparation of fluorescent ceramide

Fluorescenct ceramide was purchased from Molecular Probes, Inc. (Eugene, Or). A 1mM stock solution was prepared by dissolving the ceramide in dimethyl sulfoxide (DMSO). Aliquots of ceramide were stored frozen and in a light proof container. For a working solution, the ceramide was diluted with 0.68 mg/ml BSA in HCMF (Hepes buffer, calcium and magnesium free, pH 7.3) to a final concentration of 5μM.

B. Preparation of frozen tissue sections

One year old turkeys were sacrificed by decapitation. The pituitaries were immediately wrapped in parafilm and rapidly plunged into liquid nitrogen. The specimens were maintained in liquid nitrogen until sectioned. Ten micron thick sections were obtained by cryomicrotome (Minotone from International Equipment company, a Division of Damon, Chamber Temp. -20 to -25°F). Every two to three sections were adhered to a glass slide and stored in a light proof box at -20°C.

C. Incubation with Ceramide

Frozen sections were rinsed in HCMF for 5 min. at room temperature. Incubation with 5μM ceramide was performed for 30 min. at 4°C followed by "back exchange" with 4 changes of 0.34 mg/ml BSA in HCMF at 37°C over a period of 2 hours. The stained sections were fixed with 3% paraformaldehyde and 0.5% glutaraldehyde in 0.1M phosphate buffer for 30 min and then rinsed with HCMF. A drop of mounting medium (9:1 glycerol to PBS, pH8.0) containing 0.1 M p-phenylenediamine was placed on the sections and a coverslip was mounted on top. The edges of the coverslip were sealed with nail polish to avoid rapid oxidation. The slides were stored in a light proof box at-20°C.

D. Double Label Procedure

Frozen sections were rinsed in PBS for 5 min at RT then with 1% BSA for 5 min. at RT followed by 2% goat serum for 10 min. at 4°C before incubation with primary antibody. Incubation with primary antibody (either rabbit anti-turkey GH or rabbit anti-turkey PRL) was done overnight at 4°C. Sections were rinsed in 1% BSA and then incubated with Texas red anti-rabbit antiserum (Molecular Probes, Eugene, OR) diluted 1:40 for 1 hour at RT. Texas Red, rhodamine B type fluorachrome, was chosen as an antibody label since it resists photobleaching and has excitation and emission wavelengths that are separate from that of ceramide which has the characteristics of fluorescein. After antibody incubations were completed, the sections were processed for labeling with ceramide as described above.

E. Imaging and Photography

Fluorescence imaging was performed usign a Biorad MRC-600 confocal laser scanning microscope equipped with a Krypton-Argon laser mounted on a Nikon Optiphot microscope. Images were captured using a 60X 1.4 NA Nikon Planapo lens, a confocal pinhole setting of 0, Zoom 1.0-1.5, and a single slow scan. The laser was attenuated to 0.1% transmittance. Ceramide was imaged using the 488 nm line of the laser while Texas Red was imaged using the 568 nm line. In an area of interest, images of each fluorochrome were collected from identical optical sections. All of the iamges were stored digitally and archived to an IBM 3363 WORM drive.

Images were pseudocolored to represent the actual emission wavelength (Ceramide, green; Texas red, red). To create double label images, files form identical optical sections were merged and colorized using the Biorad software. Hardcopies of these images were obtained by photographing the computer screen using Kodak Gold 200 film.

RESULTS AND DISCUSSION

Both growth hormone (GH) and prolactin (PRL) cells are seen throughout the turkey anterior pituitary gland. There are more PRL cells than GH cells in the tissue because the animals

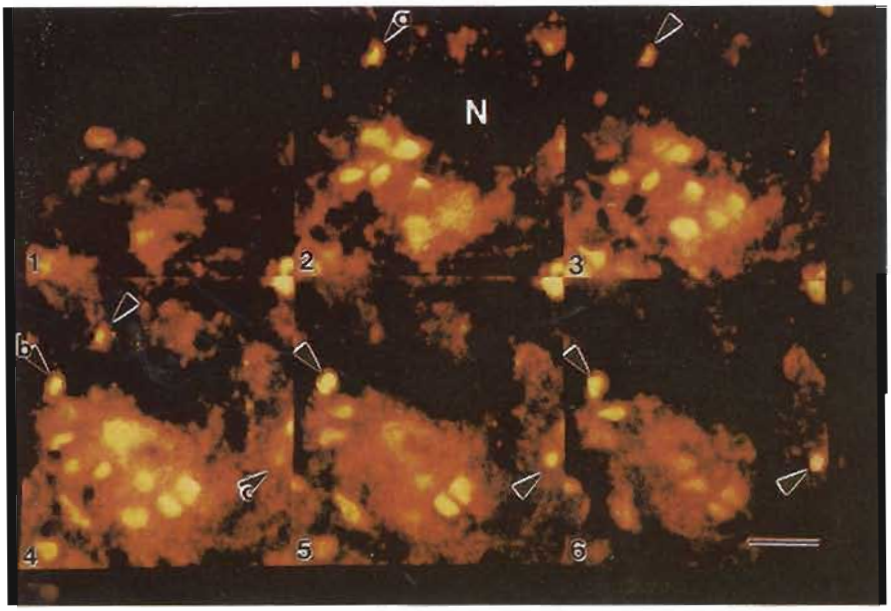

A

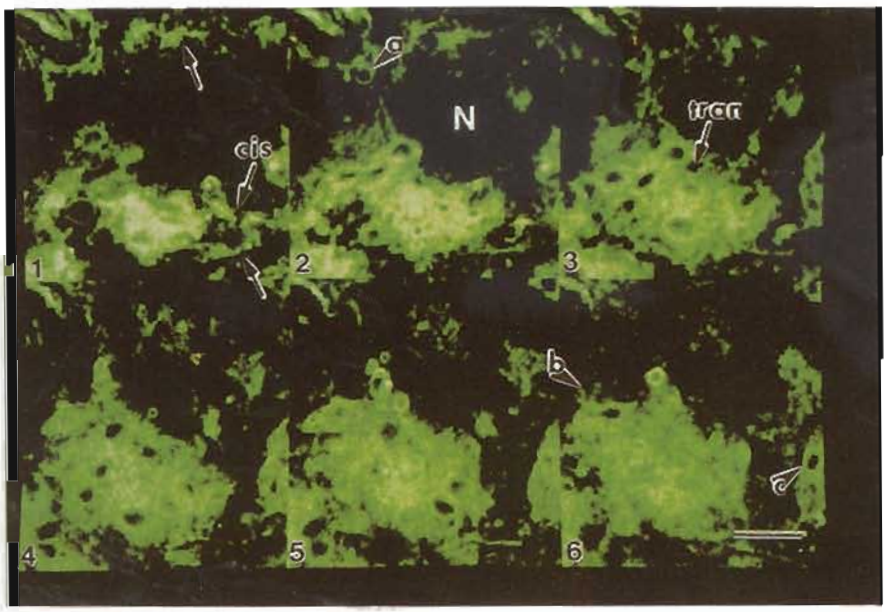

B

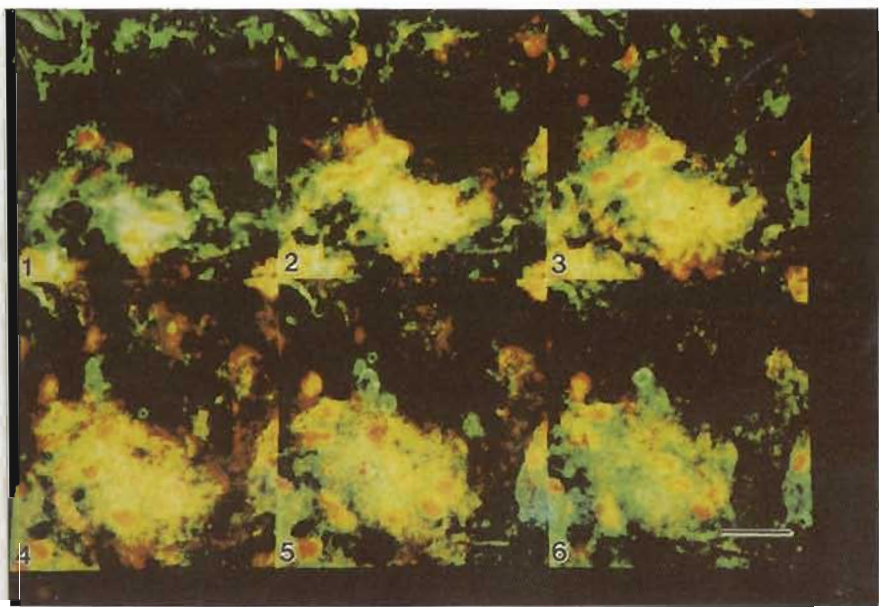

Fig. A-C
Six optical sections were collected through a section of a GH cell. Fig. A shows numerous granules labeled with anti-GH antiserum. In the same section, the Golgi forms an intricate membrane network (Fig. B). By merging and colorizing identical optical sections of each probe, Fig. C illustrates the distribution of hormone granules (orange) within the Golgi complex (green). N: nucleo. a, b: indicating where GH granules are situated within the cisternae of the Golgi.

used in this study were one year old mature laying birds.

In a series of optical sections through the section of a pituitary cell we detected numerous, large granules labeled with anti-GH (Fig. A). In the same section, the Golgi forms an intricate membrane network (Fig. B). By merging and colorizing identical optical sections of each probe we can better visualize the distribution of hormone granules within the Golgi complex (Fig. C).

The series of optical sections depicted in Fig. A-2 shows a granule appearing in panel 2 is also present in panels 3 and 4 and is absent in panel 5. This granule is approximately 480nm. Ceramide staining seen in Fig. B-2 shows that the granule is within a Golgi vesicle and may be ready for release. Granule b seen in Fig. A-4,5 and 6 is larger, measuring approximately 720nm. This could be a single granule or a cluster of granules. It appears to be in the cytoplasm not in the cisternae of Golgi (Fig. B-6). The Golgi structure seen in Fig. B forms a continuous network around the nucleus. There are a few cisternae proximal to the nucleus (Fig. B, arrows) but no granules are present. This could be the cis side of the Golgi complex. The trans Golgi network is clearly identified by the presence of granules. This part of the network is composed of numerous cisternae with cavities that gradually enlarge in diameter and contain an immunoreactive granule. In the merged images it is clearly seen that the immunoreactive granules are enveloped by the cisterne of the Golgi (Fig. C). These fluoresecent granules may be mature hormone granules within the Golgi tubule or they may be pre-secretory granules which have accumulated at ends of the trans Golgi stacks prior to release into the cytoplasm. This structure has also been observed by TEM [30] as an expanded portion of the Golgi cisterne in which numerous granuels are formed or stored. HR-SEM images show large presecretory granules [29] near the edge of the cisternae at the trans Golgi pole.

The spatial relationship of hormone granules and Golgi in PRL producing cells was also studied. In these cells the prolactin does not appear to form large discreet granules like those formed by GH. Rather, the PRL appears as small developing granules distributed throughout most of the tubular cisternae of the trans Golgi network with the larger, mature granules more prevalent near the periphery of the Golgi stack (Fig. D). Regions which lack prolactin granules are probably the cis side of the Golgi complex. As seen in the other cell type, the Golgi complex is a continuous network of interconnected cisternae surrounding the nucleus which occupies most of the cell volume (Fig. E). Fig. F is a merged image of both the prolactin staining (Fig. D) and the ceramide label (Fig. E). Overlapping signal appears yellow thus serving to illustrate that the prolactin is indeed distributed throughout the Golgi network.

CONCLUSIONS

There is no doubt that transmission electron microscopy (TEM) is still the most valuable tool for ultrastructural studies since it is unrivaled in its ability to provide high resolution images of intracellular structures. However, this high resolution information is only available for a limited volume represented in a thin section of a cell. High voltage TEM is an alternative method for imaging larger volumes of the cell in thick section (up to 1μm) but the image produced is often confused due to the presence of overlapping structures. Stereo micrography and selective staining techniques can help to clarify the images produced in the TEM, however the limitation of field of view remains. Confocal laser scanning microscopy can be used as a complementary image mode allowing (1) examination of specimens too thick for electron microscopy, (2) detection of multiple labels within one sample, (3) rapid verification of antibody immunoreactivity.

Confocal laser scanning microscopy enables one to image selectively stained material in individual optical sections with a z-resolution of approximately 0.5 μm through a depth of 100-200 μm. Excitation lines available from the laser enable the visualization of multiple fluorescent or reflective labels within the same specimen. These images can then be analyzed individually or compiled to form a 3-dimensional reconstruction of the structures. The availability of specific antibodies to hormones and Golgi specific ceramide has allowed us to take advantage of this methodology. Confocal images of turkey pituitary cells has provided us with the spatial relationship of hormone granule formation within Golgi network. We have also obtained information on the possible route of hormone secretion.

ACKNOWLEDGEMENTS

This work was supported by the Laboratory for Biological and Biomaterials Specimen Preparation, Dept. of Animal Health and Biomedical Sciences University of Wisconsin-

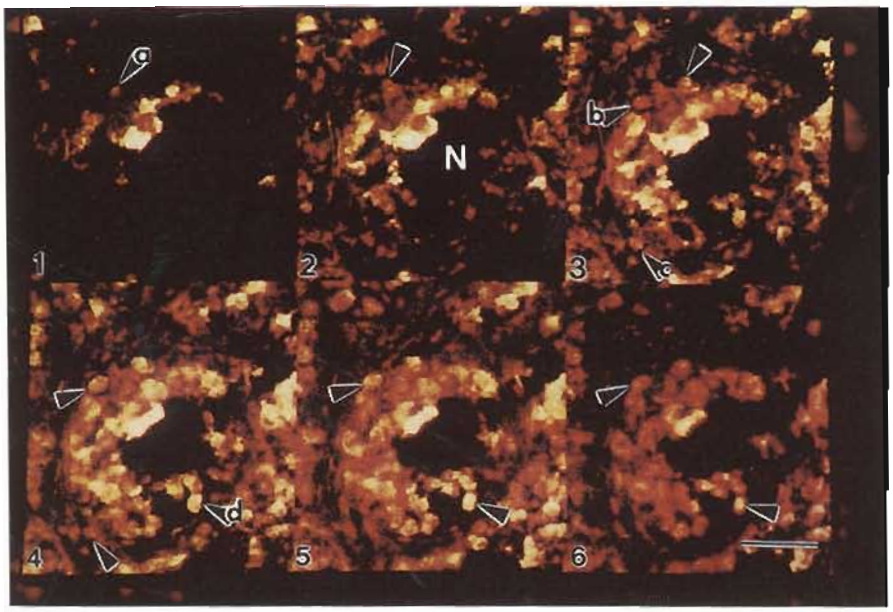

D

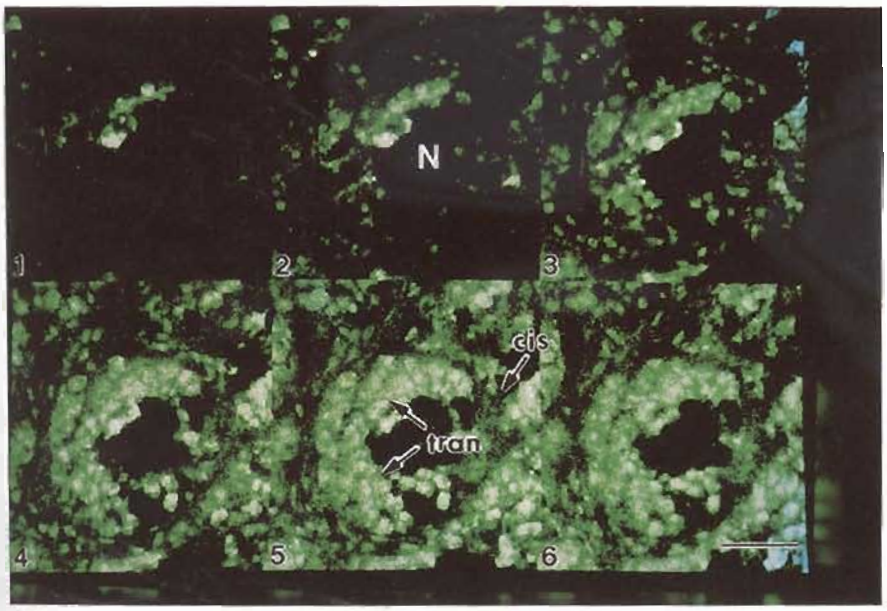

E

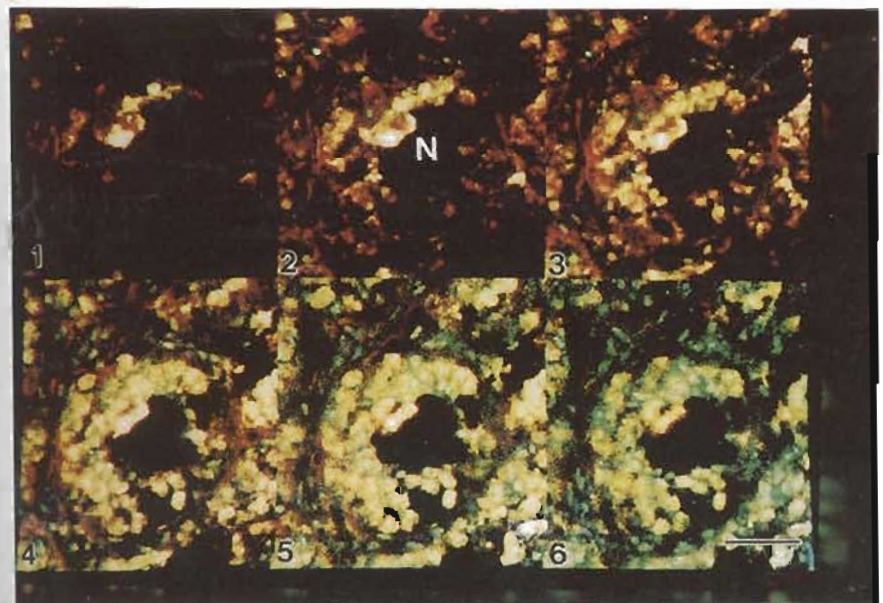

Fig. D-F
Six optical sections were collected through a section of a PRL cell. The prolactin appears as small developing granules distributed throughout most of the tubular cisternae of the trans Golgi network with the larger, mature granules more prevalent near the periphery of the Golgi stack (Fig. D). Fig. E shows that the Golgi complex is a continous network of interconnected cisternae surrounding the nucleus which occupies most of the cell section. Fig. F is a merged image of both the prolactin staining (Fig. D) and the ceramide label (Fig. E).

Madison, and Grant PI-28 of Venezuela CONICIT (Consejo Nacional de Investigaciones Científicas y Tecnológicas).

Confocal microscopy and HR-SEM were performed at the Integrated Microscopy Resource, Madison, WI a Biomedical Research Resource supported by NIH Biomedical Research Technology Grant RR 00570.

We would like to thank Mr. Paul Sims for his technical support.

RESUMEN

Cortes congelados de glándula pituitaria de pavo fueron procesadas para su observación en microscopia de barrido láser confocal (CLSM).

Se aplicó el método de doble marcaje a estas muestras congeladas. Los cortes fueron previamente incubados con un anticuerpo primario (conejo anti-hormona de crecimiento de pavo, GH, o conejo anti-prolactina de pavo, PRL) y posteriormente fueron incubados con antisuero Texas-red anti-conejo. Una vez completadas las incubaciones con los anticuerpos mencionados los cortes fueron marcados con ceramida fluorescente.

Las imágenes fluorescentes fueron obtenidas con un LSCM, estas imágenes revelan la distribución de las células GH y PRL, y además las relaciones espaciales de los gránulos de hormona y el complejo de Golgi.

REFERENCES

1. Beaudoin, A.R. and Grondin, G. (1991) Secretory pathways in animal cells: with emphasis on pancreatic acinar cells. J. Electron Microsc. Tech **17:** 51-69.

2. Bennett, G. and Wild, G. (1991) Traffic through the Golgi apparatus as studied by radioautography. J. Electron Microsc. Tech. **17:** 132-149.

3. Bergeron, J.J.M., Evans, W.H. and Geschwind, I.I. (1973) Insulin binding to rat liver Golgi fractions. J. Cell Biol. **59:** 771-776.

4. Bergeron, J.J.M., Borts, D. and Cruz, J. (1978) Passage of serumdestined proteins through the Golgi apparatus of rat liver. J. Cell Biol. **76:** 87-97.

5. Bergeron, J.J.M., Rachubinski, R.A., Sikstrom, R.A., Posner, B.I. and Paiement, J. (1982) Galactose transfer to endogenous acceptors within Golgi fractions of rat liver. J. Cell Biol. **92:** 139-146.

6. Cararro, N., Ovtracht, L. and Favard, F. (1971) Observation en microscopie electronique a haute tension de l' appareil de Golgi sur coupes de 0.5 a 5 u d' epasseur. C.R. Acad Sci. Paris Series, D, **273:** 876-879.

7. Ehrenreich, B.A. and Cohn, Z.A. (1967) The uptake and digestion of iodinated human serum albumin by macrophages in vitro. J. Exp. Med. **126:** 941-958.

8. Farquhar, M.G. (1985) Progress in unraveling pathway of Golgi traffic. Ann. Rev. Cell Biol. **1:** 477-488.

9. Farquhar, M.G. and Palade, G.E. (1981) The Golgi apparatus (Complex) - (1954 - 1981) - from artifact to center stage. J. Cell Biol. suppl. **91:** 77s-103s.

10. Fleischer, B., Fleischer, S. and Ozawa, H. (1969) Isolation and cahracterization of Golgi membranes from bovine liver. j. Cell Biol. **43:** 59-79.

11. Fleischer, B. and Smigel, M. (1978) Solubilization and properties of galactosyltrasferase and sulfotransferase activities of Golgi membranes in Triton X-100. J. Biol. Chem **253:** 1632-1638.

12. Howell, K.E., Ito, a. and Palade, G.E. (1978) Endoplasmic reticulum marker enzymes in Golgi fractions. What does this mean? J. Cell Biol. **79:** 581-589.

13. Howell, K.E. and Palade, G.E. (1982) Hepatic Golgi fractions resolved into membrane and content subfraction. J. Cell Biol. **92:** 822-832.

14. Koval, M. and Pagano, R.E. (1989) Lipid recycling between the plasma membrane and intracellular compartments: Transport and metabolism of fluorescent sphingomyelin analogues in clutured fibroblasts. J. Cell Biol. **108:** 2169-2181.

15. Kraehenbuhl, J. P., Racine, L. and Jaimieson, J.D. (1977) Immunocytochemical localization of secretory proteins in bovin pancreatic exocrine cells. J. Cell Biol. **72:** 406-423.

16. Leblond, C.P. and Bennett, G. (1976) Role of the Golgi apparatus in terminal glycosylation. In

international Cell Biology. B.R. Brinkley and K.R. Porter eds., Rockfeller Univ. Press, New York. pp. 326-336.

17. Lipsky, N.G. and Pagano, R.E. (1983) Sphingolipid metabolism in cultured fibroblasts: microscopic and biochemical studies employing a fluorescent ceramide analogue. Proc. Natl. Acad. Sci. USA. **80:** 2608-2612.

18. Lipsky, N.G. and Pagano, R.E. (1985a) Intracellular translocation of fluorescent sphingolipids in clutured fibroblasts: endogenously synthesized sphingomyelin and glucosylcerebroside analogues pass through the Golgi apparatus in route to the plasma membrane. J. Cell Biol. **100:** 27-34.

19. Lipsky, N.G. and Pagano, R.E. (1985b) A vital stain for the Golgi apparatus. Science (Wash. DC). **228:** 745-747.

20. Mollenhauer, H.H. and Morre, D.J. (1991) Perspectives on Golgi apparatus form and function. J. Electron Microsc. Tech. **17:** 2-14.

21. Neutra, M. and Leblond, C.P. (1966) Radioautographic comparison of the uptake of galactose-H3 and glucose-H3 in the Golgi region of various cells secreting glycoporteins or mucopolysaccharides. J. Cell Biol. **30:** 137-150.

22. Pagano, R.E. and Sleight, R.G. (1985) Defining Lipid Transport pathways in animal cells. Science **228:** 1051-1057.

23. Pagano, R.E., Sepanski, M.A. and Martin, O.C. (1989) Molecular Trapping of a fluorescent ceramide analogue at the Golgi apparatus of fixed cells: Interaction with endogenous lipids provides a trans-Golgi marker for both light and electron microscopy. J. Cell Biol. **109:** 2067-2079.

24. Rambourg, A. (1969) L' appareil de Golgi: examen en microscopie electronique de coupes epaisses (0.5-1 u) colorees par le melange chlorhydrique-phosphotungstiques. C.R. Acad. Sci. Paris, serie D. **269:** 2125-2127.

25. Rambourg, A. and Chretien, M. (1970) L' appareil de Golgi: examen en microscopie electronique de coupes epaisses (0.5-1 u) apres impregnation des tissus par le tetroxyde d' osmium. C.R. Acad. Sci. Paris, serie D. **270:** 981-983.

26. Rambourg, A., Clermont, Y. and Marraud, A. (1974) Three-dimensional structure of the osmium-impregnated Golgi apparatus as seen in the high voltage electron microscope. Am. J. Anat. **140:** 27-46.

27. Rambourg, A., Clermont, Y. and Hermo, L. (1979) Three-dimensional architecture of the Golgi apparatus in sertoli cells of the rat. Am. J. Anat. **154:** 455-476.

28. Tai, S. (1992) Correlative transmission electron microscopy and high resolution scanning electron microscopy studies on the fine structural organization of the chicken pituitary gland. Scan. Microsc. **6(1):** 263-272.

29. Tai, s. (1992) correlative TEM and HR-SEM studies on the fine structural organization of chicken pituitary gland. S.E. Intern. **6(1):** 263-272.

30. Tai, S. and Albrecht R.M. (1992) The 3D architecture of the Golgi complex of chicken pituitary cells. Acta Microscopica, **1(1):** 74-86.

31. Tanaka, K. and Fukudome, H. (1991) Three-dimensional organization of the Golgi complex by scanning electron microscopy. J. Electron Microsc. Tech. **17:** 15-23.